Published in final edited form as:
Brain Stimul. 2013 September ; 6(5): 777–787. doi:10.1016/j.brs.2013.03.002.

Repetitive transcranial magnetic stimulation elicits rate-dependent brain network responses in non-human primates

Felipe S. Salinas[a,*], **Shalini Narayana**[a], **Wei Zhang**[a], **Peter T. Fox**[a], and **C. Ákos Szabó**[b]

[a]Research Imaging Institute, University of Texas Health Science Center at San Antonio, San Antonio, Texas

[b]Department of Neurology, University of Texas Health Science Center at San Antonio, San Antonio, Texas

Abstract

Background—Transcranial magnetic stimulation (TMS) has the potential to treat brain disorders by tonically modulating firing patterns in disease-specific neural circuits. The selection of treatment parameters for clinical repetitive transcranial magnetic stimulation (rTMS) trials has not been rule-based, likely contributing to the variability of observed outcomes.

Objective—To utilize our newly developed baboon (*Papio hamadryas anubis*) model of rTMS during position-emission tomography (PET) to quantify the brain's rate-response functions in the motor system during rTMS.

Methods—We delivered image-guided, suprathreshold rTMS at 3 Hz, 5 Hz, 10 Hz, 15 Hz and rest (in separate randomized sessions) to the primary motor cortex (M1) of the lightly anesthetized baboon during PET imaging; we also administered a (reversible) paralytic to eliminate any somatosensory feedback due to rTMS-induced muscle contractions. Each rTMS/PET session was analyzed using normalized cerebral blood flow (CBF) measurements; statistical parametric images and the resulting areas of significance underwent *post-hoc* analysis to determine any rate-specific rTMS effects throughout the motor network.

INTRODUCTION

Transcranial magnetic stimulation (TMS) has well-established applications in basic neuroscience and promising applications in neurological and psychiatric disorders—including recent U.S. Food and Drug Administration approval for TMS use in depression and preoperative motor mapping. At present, human TMS treatment trials lack a strong theoretical basis for selecting optimal ranges for a multitude of treatment parameters—including the TMS coil's position, orientation, intensity, stimulation rate and duration.[1–3] As a result, treatment design parameters are determined *ad hoc* and lack the support of a coherent theory or model.[4] Our understanding of the underlying physiological mechanisms of action in TMS-induced brain activations is limited by the inconsistent application of these parameters.[1–3] To address this shortcoming, we developed a functional neuroimaging non-human primate (*Papio hamadryas anubis*) model.[5] The baboon's large head size, simple

*Correspondence to: salinasf@uthscsa.edu.

All authors read and contributed to the content of this article.

cortical gyrification patterns (relative to humans), and availability for repeated studies support its use for a thorough investigation of the mechanisms and important parameters underlying TMS-induced brain activations.[5]

Of all the available TMS parameters, intensity and stimulation rate have consistently demonstrated conflicting results when using either electromyography (EMG)[6–10] or imaging[4,11–16] assessments of TMS-induced brain activity. As TMS intensity increases, the size of the neuronal population above firing threshold increases—both excitatory and inhibitory neurons—due to the larger electric field strengths at the target site; these TMS-induced neuronal activations may have specific hemodynamic consequences, resulting in cerebral blood flow (CBF) changes which may be used to quantify/assess the effect(s) of certain TMS protocols.[17] Suprathreshold TMS increases both the local and remote CBF responses,[4,11,12,14,15,18,19] whereas subthreshold TMS may or may not activate the targeted network;[13,14,16] the state dependence of these networks may also be assessed.[18,19] Since many clinical TMS applications aim to modulate specific brain regions and/or networks,[20–23] the level of TMS intensity is an important determinant of whether or not we are stimulating just one node or multiple nodes in that brain network. The attractiveness of this approach can be readily appreciated in the limbic-cortical network of depression,[24–26] where nodes—i.e. subgenual cingulate—of the network may be too deep to directly stimulate (non-invasively) with rTMS, but the network may still be accessed by its more superficial nodes such as the dorsolateral prefrontal cortex (DLPFC).

rTMS rate is commonly accepted as the main determinant of whether a repetitive TMS (rTMS) intervention will be excitatory (>1 Hz) or inhibitory (≤1 Hz)[1,3]—where the assumption is that all excitatory rTMS frequencies increase brain activity in the same linear way.[6,13] However, since the visual system[27,28] (i.e. photic stimulation) and the somatosensory system[29–32] (i.e. tactile or electrical stimulation) demonstrate different frequency-dependent tuning curves, we believe that further investigation into the frequency-specific brain responses are warranted. Furthermore, we believe that once determined, these rate-responses may be used to inform treatment protocols and increase their overall efficacy, especially at the network level where some nodes may be too deep in the brain for direct TMS interactions (e.g. subgenual cingulate cortex in the depression circuit). Therefore, to impress the concept of the rate-specific “network” rTMS approach, we investigated the rate-dependence of suprathreshold rTMS on the local and remote effects of CBF in the motor system.

MATERIALS & METHODS

Animal preparation

Five normal, adult baboons (*Papio hamadryas anubis*; 4 females) with body weight of 16.4 ± 2.4 kg (mean ± SEM) were studied in accordance with the policies of the Institutional Animal Care and Use Committee of the University of Texas Health Science Center at San Antonio; this study fully complied with U.S. Public Health Service’s *Guide for the Care and Use of Laboratory Animals*[33] and the *Animal Welfare Act*.[34] Before imaging, each animal was screened for neurological disorders (i.e. epilepsy) using electroencephalographic (EEG) techniques described by Szabó *et al.*.[35] The anesthetized animal preparation—for optimized physiological stability and functional imaging responses—has been described in previous studies.[5,36] Briefly, for each imaging procedure (MRI and PET), each animal received an injection of intramuscular ketamine (5 mg/kg) to facilitate oral intubation and catheterization of a venous delivery line; intramuscular atropine (0.3 mg) was administered to reduce oropharyngeal secretions. During each imaging session, we maintained sedation with continuous i.v. administration of ketamine (5–6 mg/kg/hr) and vecuronium (0.25 mg/kg/hr) —a paralytic that acts at the neuromuscular junction. Upon conclusion of the imaging

session, we administered atropine (0.6–1.2 mg, i.v.) and neostigmine (0.5–2.0 mg, i.v.) to reverse muscle paralysis. During the entire procedure, the animals' respiration, heart rate and oxygenation were monitored.

TMS image-guidance

All TMS delivery was image-guided, utilizing high-resolution structural and functional magnetic resonance images (fMRIs) using previously described techniques.[5,36] All MRIs were performed on a Siemens TIM-Trio 3T clinical scanner using a body radiofrequency (RF) transmission coil with a 12-channel head RF receiver coil (Siemens, Erlangen, Germany). We obtained high-resolution anatomical images using an MP-RAGE sequence (TR/TE/ ip angle = 2300 ms/3.66 ms/13°) with slice-select inversion recovery pulses (TI = 751 ms), FOV = 128 mm × 128 mm × 80 mm, and 0.5 mm isotropic spatial resolution. We used the anatomical MRIs for co-registration between imaging modalities (MRI and PET) in order to register each animal's $H_2{}^{15}O$ PET images to their native MRI then warp them to a representative baboon's MRI brain space.

Blood-oxygen-level dependent (BOLD) fMRI was acquired using gradient-echo, echo-planar imaging (EPI; TR/TE = 2.5 s/30 ms), FOV = 150 mm × 150 mm × 48 mm, and spatial resolutions of 1.5 mm × 1.5 mm × 4 mm. Somatosensory stimulation was applied to the animal's right hand via a custom-made pneumatic-driven vibrotactile stimulator;[36] vibrotactile stimulations were applied—at a stimulation frequency of 5 Hz—using an 50 second on/off block design. We processed the fMRI data using the FEAT toolbox[37] in the FMRIB's Software Library (FSL).[38] The resulting fMRIs were utilized to determine the location of each baboon's primary sensory cortex representation of the right hand ($S1_{hand}$). The $S1_{hand}$ and primary motor cortex representation of the hand ($M1_{hand}$) representations lie directly across the central sulcus from one another.[39] Therefore we determined each animal's $M1_{hand}$ location (i.e. target location) to be the site in the precentral gyrus which is adjacent to that animal's $S1_{hand}$ fMRI activation. We validated this approach in our previous baboon TMS/PET study.[5]

rTMS

We used a MagPro Cool-B65 figure-of-eight rTMS coil connected to a MagPro R30 Magnetic Stimulation Unit (MagVenture A/S, Farum, Denmark) for each rTMS procedure. The TMS coil's site of maximal electric field (E-field) induction (i.e. "hot spot") was determined using methods developed by Salinas *et al.*[40,41] These articles describe techniques through which we measured and modeled the E-field vectors induced by each TMS pulse. Using each animal's fMRI map of the $S1_{hand}$ and the corresponding target locations for $M1_{hand}$, we determined the scalp location closest to the $M1_{hand}$ site, then measured the distances from this scalp location to specific anatomical landmarks (nasion, inion, earholes). Finally, we stereotactically positioned the TMS coil over each animal's left primary motor cortex ($M1_{hand}$), while lying supine in the PET scanner, so that the location of the TMS coil's maximum induced E-field coincided with the targeted M1 location (Fig. 1A). Once positioned, the orientation of the TMS coil—i.e. the E-field and current direction—was adjusted to be perpendicular to the animal's central sulcus (with the E-field directed antero-medially, towards the animal's snout); this approach is consistent with the cortical column cosine (C3) aiming theory proposed by Fox *et al.*.[4] We applied single pulses of TMS to each baboon's left $M1_{hand}$ to visually establish each animal's resting motor threshold (RMT) at the first dorsal interosseous (FDI) muscle of the contralateral hand; the RMT was defined as the minimum intensity of stimulation capable of producing FDI muscle contractions in at least 5 out of 10 trials. Once each baboon's RMT was found, a one-time bolus injection of vecuronium was given to eliminate movement throughout the rTMS/PET session.

Each baboon underwent rTMS at stimulation frequencies of 3 Hz, 5 Hz, 10 Hz and 15 Hz. rTMS pulses were delivered to $M1_{hand}$ at 120% RMT during concurrent $H_2{}^{15}O$ PET scans. Each rTMS frequency was delivered at least 30 seconds prior to the injection of ^{15}O-labeled water and continued until 60 seconds after the injection (Fig. 1B). The number of rTMS pulses delivered at each stimulation frequency was held constant at 450 pulses (e.g. train duration varied across frequencies); this was done to decrease any possible dose effects—which may alter the excitability state of the motor cortex.[9,11] The 3 Hz rTMS frequency was continuously applied 90 seconds prior to radiotracer injection and continued for 60 seconds afterward, for a total 3 Hz rTMS duration of 150 seconds. The 5 Hz rTMS frequency was also continuously applied, but began only 30 seconds prior to radiotracer injection and continued for 60 seconds afterward, for a total 5 Hz rTMS duration of 90 seconds. The 10 Hz rTMS frequency was applied intermittently in 5 second trains with 5 second inter-train intervals, whereas the 15 Hz rTMS frequency was applied intermittently in 5 second trains with 10 second inter-train intervals; the 10 Hz and 15 Hz rTMS pulse trains began 30 seconds prior to radiotracer injection and continued for 60 seconds, for a total rTMS duration of 90 seconds (e.g. 450 pulses for each rTMS frequency). The order of stimulation frequencies was randomized and a rest condition was used to represent the baseline scan.

In this experimental design we did not employ a sham condition because we did not know *a priori* what (if any) effect rTMS frequency may have on the auditory cortex, thus we would need corresponding sham rTMS frequency conditions for each rate being investigated. These sham conditions would have drastically increased scan times and the period required for animal sedation (and chemically-induced paralysis) during each imaging session. In addition, because we were not investigating any treatment effects during this acute application of rTMS, we did not anticipate any placebo effects due to rTMS in our baboon model. The combinations of rTMS frequency, stimulus duration, and TMS intensity fall within published rTMS safety guidelines.[42–44]

A separate study comparing the effects of rTMS dose was also performed to assess whether or not the number of rTMS pulses applied affects CBF throughout the motor system (Fig. 1C). For this study, we applied 3 Hz rTMS intermittently in on/off 5 second-trains for a total of 225 rTMS pulses. We selected 3 Hz rTMS as our frequency of interest for the following reasons: 1) our prior research with 3 Hz rTMS[4,45] successfully produced reliable TMS-induced brain activations, 2) we did not have *a priori* knowledge of the optimum network frequency, and 3) technical issues such as coil heating were easily managed by using a lower rTMS frequency.

Electroencephalography

We performed EEG recordings throughout each rTMS/PET session to monitor the level of sedation and any possible onset of seizure activity. The EEG unit used in this study was not TMS-compatible therefore we did not analyze the resulting EEG waveforms for real-time TMS-induced effects. After the baboons were sedated, we positioned eight cephalic electrodes for each rTMS session (FP1, FP2, T3, C4, O1, O2, ground and reference sites)—using the 10–20 EEG system—with EEG electrode paste and secured them with collodion-soaked gauze strips. The electrodes were connected to a portable, laptop-based EEG acquisition machine (Nihon-Kohden, Tokyo, Japan) which enabled real-time monitoring of the EEG waveforms (when the signal was not contaminated by rTMS artifacts); in addition to online EEG monitoring, the EEG results of each rTMS/PET session were also reviewed (*ex posto facto*) by a board-certified clinical neurophysiologist (C.Á.S.).

Positron emission tomography

PET data were acquired with a CTI EXACT HR+ scanner (Knoxville, TN). Sixty-three contiguous slices (2.5 mm thick) were acquired in a transaxial plane of 128 × 128 voxels with a 2 mm in-plane voxel resolution. Images were corrected by measured attenuation using 68Ge/68Ga transmission scans and reconstructed at an in-plane resolution of 7-mm full width at half maximum (FWHM) and an axial resolution of 6.5-mm FWHM. Water labeled with oxygen-15 ($H_2{}^{15}O$, half-life of 122 s) was administered intravenously—370 MBq $H_2{}^{15}O$ dose/scan—and cerebral blood ow (CBF) was measured using a bolus technique.[4] We applied each condition (high-frequency rTMS or rest) once during each PET session. We immobilized each baboon in the PET scanner using a custom-made, padded animal restraint.[5]

Data analysis

We performed image preprocessing using previously validated methods and in-house software.[4] PET images were reconstructed into 60 slices (2 mm thick) with an image matrix size of 60 × 128 × 128, using a 5 mm Hann filter resulting in images with a spatial resolution of approximately 7 mm (full-width at half-maximum (FWHM)). PET images were corrected for head motion using the MCFLIRT tool[46] in FSL; the PET and MRI images were spatially transformed to a representative baboon's MRI brain space and co-registered using the Convex Hull algorithm.[47] Regional tissue uptake of ^{15}O-water was value normalized to a whole-brain (global) mean of 1000 counts.

Each frequency comparison was analyzed using voxel-wise statistical parametric images (SPIs). Group z-score images (SPI{z}) were obtained by contrasting each animal's task state (i.e. all rTMS frequencies) and control state (i.e. rest) using the pooled standard deviation. The objective of the analysis was to determine the locations of the M1 response induced by rTMS (at all frequencies) and its connected regions. All *p*-values were Bonferroni corrected for multiple comparisons. Only Z scores corresponding to $p \leq 0.01$ (corrected) are reported in this study.

ROI statistical analysis

Region of interest analyses[48] were performed at sites identified by the SPI{z} that were known to be associated with the motor system: M1, premotor, supplementary motor area (SMA), cingulate motor area, thalamus, striatum and cerebellum. We also investigated ROIs in the frontal and parietal areas, which were consistent with previous motor system studies.[49,50] The ROIs were determined using the Research Imaging Institute's (RII, UTHSCSA) Multiple Image Processing Station (MIPS) and visualized in its free image browser Multi-Image Analysis GUI (MANGO; available at rii.uthscsa.edu) with a 3 mm × 3 mm × 3 mm search cube. A repeated-measures one-way analysis of variance (ANOVA) was used for the initial frequency analysis of the rTMS studies. For comparisons found significant by ANOVA, Newman-Keuls *post-hoc* tests were performed to determine which frequencies demonstrated significant differences.

RESULTS

We monitored sedation level and seizure activity (via EEG) during each animal's rTMS/PET session and found no instances of oversedation, ictal, interictal, or abnormal brain activity. Since each animal was lightly-sedated throughout each PET session, there were no significant changes in their EEG waveforms during or immediately after each rTMS protocol (e.g. there was no increase in arousal following rTMS). After each imaging session, we recovered and monitored each animal for a period of one hour. During this period, each animal exhibited normal behavior—including regular food intake and activity level. No

animals demonstrated any evidence of adverse effects of rTMS during (or after) their respective imaging sessions.

Motor network connectivity

The rTMS/PET study demonstrated significant activations (Fig. 2) in the targeted $M1_{hand}$ area, the premotor cortex, caudate, and the contralateral supplementary motor area (SMA), cingulate motor area, and cerebellum for all implementations of high-frequency rTMS. There were also significant deactivations in the contralateral thalamus; each of these regions is associated with the motor system and our results were consistent with previous reports of motor network connectivity. [49–58] All of the locations are listed in Table 1; where homologous brain regions were labeled using a rhesus atlas.[59]

Frequency effects in the motor network

Region-specific rate-responses for each rTMS stimulation frequency were shown in Fig. 3. An ANOVA revealed significant activations during rTMS when compared to the baseline ROI value for each of these regions and the results are listed in Table 2. Newman-Keuls *post-hoc* analyses revealed that at the target site (left M1), only the 5 Hz and 15 Hz rTMS frequencies demonstrated significant differences from the resting CBF levels. All frequencies demonstrated significant activations in the premotor cortex, caudate and the cerebellum (Fig. 3; Table 2). In the premotor cortex and cerebellum there were no significant differences between each rTMS frequency, whereas in the caudate there were significant differences between frequencies (Fig. 3; Table 2). In the SMA, only the 5 Hz rTMS frequency demonstrated significant differences from the resting CBF levels (Fig. 3; Table 2). In the cingulate motor area, only the 5 Hz and 10 Hz rTMS frequencies demonstrated significant differences from the resting CBF levels, whereas there were also significant differences between frequencies (Fig. 3; Table 2). In the thalamus, all rTMS frequencies demonstrated significant differences from the resting CBF levels (Fig. 3; Table 2), however only the 5 Hz and 15 Hz rTMS frequencies were significantly different from the other rTMS frequencies. The majority of these regions exhibited system-wide, linear responses with frequency up to the 5 Hz peak followed by decreases at higher frequencies, suggesting that the motor system is tuned to the 5 Hz frequency. In addition, although many studies have reported inhibitory brain activity to the contralateral M1 region during rTMS,[11,12,14] we found no significant CBF changes at any rTMS frequency in the homologous contralateral $M1_{hand}$ region (Fig. 2–3; Table 2).

Responses in other brain areas during rTMS to M1

Many previous studies have found anatomical connections between the motor and cingulate motor area in the macaque monkey.[60–63] These studies found that the cingulate cortex had numerous connections to the DLPFC, the insular cortex, and area 7 of the parietal lobe. Our results in the baboon demonstrate significant activations in each of these brain regions; see Table 1 and Fig. 2. We observed brain activity in the prefrontal/frontal area in the DLPFC, insular cortex, parietal operculum and the anterior intraparietal area (AIP). Region-specific rate-responses for each rTMS stimulation frequency were shown in Fig. 4 and the initial ANOVA results for these regions are listed in Table 2.

Post-hoc tests indicated that the DLPFC activations demonstrated significant activations at all rTMS frequencies (except at 15 Hz); all rTMS frequencies were also significantly different from the 15 Hz rTMS scan at the DLPFC during M1 stimulation (Fig 4). In the insular cortex and the parietal operculum, all rTMS frequencies were significantly different from the resting CBF levels (Fig. 4), however only the 5 Hz rTMS frequency was significantly different from the other rTMS frequencies. In the AIP, all rTMS frequencies

demonstrated significant differences from the resting CBF levels, however only the 5 Hz and 15 Hz rTMS frequency were significantly different from each other (Fig. 4).

Additionally, the primary auditory cortex (A1) exhibited a saturated CBF response at all rTMS frequencies with no significant differences between rTMS frequencies. Thus, future studies may not need to account for auditory rTMS rate effects when delivering sham rTMS. However, factors such as sham TMS intensity (i.e. loudness) and local skin sensations created by active rTMS may still be potential confounds when examining TMS-induced brain activations.

Number of stimuli vs. frequency

We also delivered 3 Hz rTMS (continuously and intermittently) to ensure that the number of rTMS pulses delivered during each 90-second rTMS session did not have an cumulative effect on CBF (Fig. 5A). Although the continuous and intermittent 3 Hz rTMS sessions are not significantly different from the resting CBF value in L-M1, when comparing intermittent and continuous 3 Hz rTMS at every location listed in Table 1, a very significant ($p < 0.0001$) linear relationship exists between them (Fig. 5B). Therefore, at these session durations (90 seconds), we believe that the number of stimuli (i.e. ≤ 450 pulses) and the intertrain interval (5 seconds) in the intermittent 3 Hz rTMS sessions were not as important as the frequency of the stimulation on local changes in CBF.

DISCUSSION

Stimulation rate is commonly accepted as the main determinant of whether rTMS will be excitatory (> 1 Hz) or inhibitory (≤ 1 Hz)—where the assumption is that all excitatory rTMS frequencies increase brain activity in the same monotonic (i.e. linear) way.[6,13] In this respect, we believe that a generic “high-frequency” or “low-frequency” approach to rTMS is inadequate, since specific brain networks (e.g. the visual and somatosensory system) demonstrate frequency-dependent tuning curves.[27–32] Also, by using functional neuroimaging instead of an electrophysiological approach, we are focusing on the *brain’s* response to TMS, thus neglecting any ambiguous contributions from the spinal cord or any other parts of the peripheral nervous system. In this study, we investigated the motor system’s CBF responses to various rTMS frequencies. The targeted M1 demonstrated its largest rTMS-induced brain activations at a 5 Hz stimulation frequency. Rather than a plateau effect (i.e. saturation) at higher stimulation frequencies, we found significant decreases in CBF throughout the motor network. This unimodal frequency-dependence was observed at both local and remote brain regions at sites known to be associated with the motor network.

Motor network responses

While there were significant frequency responses in the targeted $M1_{hand}$ region (Fig. 3), the variability of the CBF responses to rTMS in this region should be discussed. It is important to note that each animal’s M1 region was determined and targeted on a per-subject basis, inherently introducing variability in the targeted M1 location. When spatially normalizing for group comparisons, the assumptions were: 1) that the target site for each of these animals would be in the same location and 2) that the TMS coil (i.e. the induced E-field vector) would be oriented in the same manner for each animal. Although the topography of the baboon’s M1 region is more consistent than in human subjects,[5] there were slight variations in the target locations of each baboon. Regardless of frequency-dependence, if each animal’s target location were different, then their group SPI{z} may be dampened due to a locally distributed CBF response. In addition to stereotactic mismatches, at suprathreshold rTMS intensities there are other complex issues to consider. As the stimulation intensity increases

the size of the neuronal population—both excitatory and inhibitory neurons—above firing threshold also increases. Thus, by stimulating each animal's target $M1_{hand}$ location at suprathreshold rTMS intensities, we may also be measuring an inherently diminished CBF response at the local M1 target site. However, by using a suprathreshold rTMS intensity we also activated remote regions—which are connected to the target location. We observed less variation in the CBF changes at the remote sites indicating that the effect of this activity was more specific at these remote sites.

While it is commonly accepted that low-frequency (i.e. ≤ 1 Hz) rTMS decreases cortical excitability to the contralateral M1, there have been few reports of suprathreshold high-frequency rTMS effects on the contralateral M1 site.[64] Previous EMG studies have reported conflicting effects due to cortico-cortical connections with the contralateral M1 site (see Fitzgerald *et al.*[1] for a review). Neuroimaging studies of rTMS effects have also reported mixed results on contralateral M1 activity[11,12,14–16,65] at different rTMS frequencies and intensity ranges. In this study, the contralateral M1 hand region did not demonstrate significant brain activity at any of the rTMS frequencies used in this study (Fig. 3); although the contralateral M1 leg area appears to be inhibited (Fig. 2). This may also be a result of the per-subject targeting of M1—as is evident in the large errors of the group-wise contralateral M1 rate data (Fig. 3). Some researchers have reported increases in CBF to the contralateral M1 at suprathreshold intensities, even when using low-frequency rTMS.[15] It is plausible that more consistent application of rTMS to the target M1 site may have produced significant activations at the contralateral M1 site. Another explanation for the lack of contralateral M1 hand inhibitions may be that those connections are tuned to lower (i.e. 1 Hz) rTMS frequencies.

Interestingly, we found a deactivation of the contralateral thalamus (also tuned to 5 Hz rTMS), however, we do not know if this deactivation was due to thalamo-cortical or cortico-thalamic fibers. One possible explanation for the decreased activation in the contralateral thalamus may be increased arousal due to rTMS. However, since each animal remained lightly sedated throughout each imaging session and we observed no increases in EEG activity (e.g. rTMS-induced arousal) following each rTMS protocol, this possibility appears highly unlikely in our current study. It is plausible that deactivation of the contralateral thalamus may be the result of the ipsilateral M1 inhibiting the contralateral M1 (via transcallosal connections) then transferring this inhibitory response to the contralateral thalamus; again, inhibition (or lack thereof) of the contralateral M1 may have been affected by the subject-specific targeting of the motor cortex (described above). Another possibility would be that the ipsilateral M1 communicates directly with the contralateral thalamus via cortico-thalamic crossing fibers. Either way, the deactivation of the contralateral thalamus is strongest at 5 Hz rTMS—the frequency at which the motor network appears to be tuned. Di Lazzaro et al.[66] suggested that 5 Hz rTMS can selectively modify the excitability of GABAergic inhibitory networks in the motor cortex. We believe that a decrease in GABAergic contributions from the thalamus may be responsible for (at least) part of the increased activation of the ipsilateral M1, however more research must be performed to investigate this further.

Non-motor responses

If we are exclusively trying to target the motor network, recruitment of non-motor brain regions may decrease the efficacy of a network-based TMS treatment protocol. Activity in these non-motor regions may be counter-productive or even deleterious to the treatment outcome. By simply decreasing TMS intensity (ex. 120% RMT to 110% RMT), we may reduce the number of indirectly connected neurons which are above firing threshold, while still activating the pertinent motor network's nodes.

Motor network rate effects

We observed frequency-dependent CBF responses throughout the motor network with a unimodal frequency distribution peaking at 5 Hz rTMS (Fig. 3). At higher rTMS frequencies, the measured CBF responses decrease at each of the motor network nodes. This behavior may be explained by GABAergic intracortical effects inhibiting the CBF response. For example, Modugno *et al.*[7] reported that short trains (4 pulses) of 5 Hz rTMS at 130% RMT resulted in inhibition, whereas longer trains (20 pulses) resulted in facilitation. Thus, the time constant for facilitatory stimulation was longer than that of inhibition. As a result, the interval between successive rTMS pulses may be too short for the motor network to fully recover when the stimulus frequency is greater than 5 Hz (as the facilitatory time constant is approached and/or passed), whereas the inhibitory network effects have fully recovered due to their shorter time constant. Previous EMG studies[6,67] demonstrated similar excitatory and inhibitory effects in motor evoked potentials when delivering TMS at similar intensities and interstimulus intervals (i.e. frequency).

It should be noted that the premotor, cerebellum and DLPFC nodes appear to have peaks at 3 Hz rather than the 5 Hz peak found in the other network nodes; the thalamus and caudate also apparently have a second (albeit lower) peak at 15 Hz (Fig. 3). Discordance with the motor network's observed rate effects may be (partially) explained by the diverse connections and functions of these respective areas. Numerous feedback loops and connections to other non-motor networks may skew the frequency-response profiles of these nodes (specifically in the subcortical nodes). Another possibility is that these cortical areas are actually communicating with M1 at a different optimal frequency (3 Hz); this suggests the rather interesting concept of sub-specificity within the motor network. However, further research must be done on the frequency-dependency of each of these nodes for a better understanding of this discrepancy.

Frequency-specific network responses

The concept of frequency-specificity in the brain is by no means novel—as it has been demonstrated in numerous research studies for several decades.[68] Recent studies have investigated the instrinsic oscillatory patterns of the brain using rTMS and electroencephalographic (EEG) techniques[69,70] during cognitive tasks; however, since EEG has poor spatial resolution, topographic mapping of frequency-dependence in rTMS/EEG studies remains inconclusive. Feurra and colleagues[71] applied transcranial alternating current stimulation (tACS) to the motor cortex at 5, 10, 20 and 40 Hz and found that only the 20 Hz stimulation increased corticospinal excitability (measured with EMG), where the lack of tACS-induced effects at the other (θα and γ) frequencies may actually be the result of using a sinusoidal tACS stimulus to entrain non-sinusoidal brain rhythms (e.g. the Rolandic central mu rhythm). Although these state-dependent effects are important, they do not reflect a brain network phenomenon but rather the peripheral motor output.

The frequency-dependent network approach to rTMS (measured with functional neuroimaging) is itself unexplored territory. While most rTMS imaging studies focus on the local—i.e. the target site's—induced brain activity, we believe that frequency-dependent changes in CBF throughout the nodes of a specific brain network offers practitioners (and researchers alike) a novel approach to non-invasive brain stimulation. For example, the frequency-selective entrainment of remote nodes in the targeted brain network has great potential for non-invasive brain therapies of neurological and psychiatric disorders—especially when the affected nodes are too deep to be directly targeted by rTMS (e.g. subgenual cingulate cortex in the depression circuit[24,25]). In addition, by analyzing the frequency-dependence of low-frequency (i.e. inhibitory) rTMS protocols on CBF changes in

specific brain networks we may also find frequency-dependent inhibitory networks—which would be beneficial in stroke rTMS studies.[22,23]

The frequency-dependence of remote nodes of specific brain networks may be exploited to increase the efficacy of non-invasive brain stimulation therapeutic protocols. By delivering suprathreshold rTMS we are stimulating the "network" and not just the targeted site. We believe that this may be an underdeveloped aspect of non-invasive brain stimulation, since it may be used to deliver rTMS pulses to deeper brain regions via their network connectivity.[26]

Number of stimuli

Although, it seems logical to conclude that simply delivering more stimulation pulses (i.e. by increasing frequency) over a specific period of time would increase CBF responses, there appears to be an upper limit to this frequency-dependent CBF response when controlling the number of rTMS pulses. We believe that by controlling the number of delivered pulses we are examining the true rate-dependent nature of the motor network. However, it should be noted that previous (non-TMS) rate effect studies of the rodent[29,31,32] and human[30] somatosensory cortices reported mixed results on whether or not the number of stimuli delivered to a brain system was the most important factor in determining the amount of neuronal activity (i.e. CBF changes) elicited. Most of these studies[29,30] suggested that although there is a linear response up to the peak (4–5 Hz in somatosensory cortex), CBF becomes saturated at higher frequencies—due to an evenly-distributed frequency response across the stimulated neuronal population.[29] Others countered[31,32] —and we concur—that CBF changes reflect "integrated rather than average neuronal activity" and when the number and duration of the stimuli are controlled, frequency-dependence arises as the chief parameter for neuronal specificity. In contrast, Fox & Raichle[27] reported the frequency-dependent nature of the human visual system to be independent of the number of photic stimuli; however, the nature of the stimulus may also be a factor in our observed CBF responses since photic and somatosensory stimuli are delivered and processed indirectly whereas TMS directly activates the cortical site.

Our results indicate that rTMS frequency, not the number of stimuli, is the main determinant of rTMS induced CBF changes in the motor network. Since the 3 Hz rTMS comparison revealed no significant differences between 225 and 450 pulses, we must conclude that frequency is the dominant factor on measured CBF changes (at least at these train durations and number of pulses). However, at higher rTMS frequencies, longer train durations and/or different inter-train intervals, the relationship between number of pulses and frequency may be more complex.[1,9,10,16] For example, Huang *et al.*[72] found that continuous theta burst stimulation (TBS) produces lower electrophysiological responses than intermittent TBS when delivered TBS in 5 Hz trains. Similarly, Rothkegel *et al.*[73] found that 5 Hz rTMS delivered in intermittent trains induces facilitative EMG results whereas continuous 5 Hz rTMS are inhibitive. As an aside, by intermittently delivering the higher rTMS frequencies used in this study, we should have seen larger CBF changes at these higher frequencies (assuming that TMS-induced CBF and EMG responses are coupled[17]). Since these higher frequencies did not produce larger CBF responses, even though they were delivered intermittently, we believe this provides more evidence that 5 Hz is the optimum rTMS frequency for the motor network. These effects, especially at suprathreshold rTMS intensities (where network effects may be assessed), need to be explored in future studies.

Benefits of the baboon model of rTMS

On of the major advantages of the baboon TMS model is the ability to use a paralytic (vecuronium) while investigating TMS-induced brain activations. In humans, upon

stimulating M1 (especially at suprathreshold TMS intensities), cortico-cortical fibers between M1 and somatosensory cortices and/or afferent feedback would facilitate the corresponding brain activity in somatosensory cortex. In the baboon, the use of a paralytic eliminated: 1) motion during the $H_2{}^{15}O$ PET imaging session and 2) any afferent feedback to the sensorimotor cortex due to TMS-induced muscle contractions. Therefore, in this baboon rTMS study, the brain activations at the targeted M1 site exhibit more realistic motor activations than in other rTMS studies.[5] Previous studies[13,14,16] utilized subthreshold rTMS intensities to decrease the effect of these afferent feedback loops; these feedback loops may confound the results of a motor rTMS study, since afferent feedback may also contribute to the state-dependence of M1. Although the use of subthreshold intensities does decrease afferent feedback (i.e. possible state-dependent effects[18,19]), it cannot reliably activate brain areas distant from the site of stimulation. Therefore, using a paralytic, we successfully applied suprathreshold rTMS intensities—activating both local and remote sites—without introducing any afferent feedback effects.

Limitations

One disadvantage of the baboon TMS model is the need for anesthesia. We have investigated the effects of ketamine on regional and global CBF measurements[5,33,70,71] and at these relatively low doses we have not found any anesthesia effects on CBF—either globally or locally. Långsjö *et al.*[74] found that ketamine induces a global, concentration-dependent increase in CBF with the largest increases in the anterior cingulate, thalamus, putamen, and frontal cortex. However, at our dosage levels we have not observed any ketamine-induced effects on CBF in our previous studies.[5,36,75] By maintaining the levels of ketamine (5–6 mg/kg/hr) throughout each $H_2{}^{15}O$ PET session we can mitigate any possible anesthesia-induced CBF effects, therefore, the CBF differences reported here are valid and not due to anesthesia effects.

Future Directions

We are currently investigating the effects of TMS on the electrophysiological[76,77] and CBF[78] responses in our baboon model of TMS. To affirm and expand these initial frequency-specific results, we plan to investigate the effects of train duration and inter-train interval on both the peripheral muscle activity (via EMG) and the brain's network responses (via functional neuroimaging) in our baboon model of TMS. Investigations into the effects of rTMS train duration on CBF at different rTMS frequencies (and intensities) may be correlated with EMG activity and used to elucidate the central and peripheral contributions in the mechanism(s) of TMS-induced brain activity.

In addition to our baboon validations of TMS' effects on the motor network, we are also investigating the use of functional connectivity to develop optimized targets for TMS delivery in other brain networks.[79] Although an anesthetized baboon model may not be used to perform a task (e.g. working memory), to identify higher-order, non-primary brain areas we may utilize region-seeded and/or independent component analyses of resting-state fMRI data (i.e. resting-state networks) to target these areas; resting-state networks can be readily identified in anesthetized non-human primates. Human and non-human primate resting-state networks appear quite similar[80] suggesting that functional locations (cyto-architectonic regions) can be targeted by their resting-state network's connectivity patterns.

CONCLUSIONS

We have demonstrated that suprathreshold rTMS may be used to non-invasively drive brain networks and that these networks exhibit frequency-specific CBF responses. We would argue—based on our results—that this frequency-dependence could be interpreted as

"network" specificity, since each node of the network demonstrates similar frequency-tuning curves, however each network may have different peak frequency. Therefore, by characterizing a specific network's (i.e. CBF) frequency-response we may then deliver more efficient, targeted, non-invasive brain therapies.

Acknowledgments

The study was funded by National Institute of Neurological Disorders and Stroke (NIH/NINDS R21 NS065431, C.Á. Szabó. Additional funding for this research came from the NIH/NINDS R21 NS062254, P.T. Fox. Dr. Salinas was supported by a Ruth L. Kirschstein National Research Service Award from the National Institute of Neurological Disorders and Stroke (NIH/NINDS F32 NS066694). The authors would like to thank Lisa Jones and Dr. Michelle Leland for performing the animal handling and sedation protocols. We would like to thank Dr. Timothy Duong, Dr. Hsiao-Ying Wey, Dr. John Li, Betty Heyl and Jesse Usrey for image acquisition and additional primate support. We would also like to thank Dr. Jack Lancaster for his helpful discussions and Crystal Franklin for image processing assistance. Drs. Szabó, Narayana, Salinas, Zhang, and Fox developed/implemented the imaging and rTMS protocols. Dr. Salinas wrote the article and performed all image/data processing. Drs. Salinas, Szabo, Narayana, and Fox performed the analysis and interpretation of the data.

References

1. Fitzgerald PB, Fountain S, Daskalakis ZJ. A comprehensive review of the effects of rTMS on motor cortical excitability and inhibition. Clinical neurophysiology. 2006; 117(12):2584–2596. [PubMed: 16890483]
2. Siebner HR, Bergmann TO, Bestmann S, et al. Consensus paper: combining transcranial stimulation with neuroimaging. Brain Stimul. 2009; 2(2):58–80. [PubMed: 20633405]
3. Pell GS, Roth Y, Zangen A. Modulation of cortical excitability induced by repetitive transcranial magnetic stimulation: Influence of timing and geometrical parameters and underlying mechanisms. Progress in Neurobiology. 2011; 93(1):59–98. [PubMed: 21056619]
4. Fox PT, Narayana S, Tandon N, et al. Column-based model of electric field excitation of cerebral cortex. Hum Brain Mapp. 2004; 22(1):1–14. [PubMed: 15083522]
5. Salinas FS, Szabó CÁ, Zhang W, et al. Functional neuroimaging of the baboon during concurrent image-guided transcranial magnetic stimulation. NeuroImage. 2011; 57(4):1393–401. [PubMed: 21664276]
6. Pascual-Leone A, Valls-Sole J, Wassermann EM, et al. Responses to rapid-rate transcranial magnetic stimulation of the human motor cortex. Brain. 1994; 117(Pt 4):847–58. [PubMed: 7922470]
7. Modugno N, Nakamura Y, MacKinnon CD, et al. Motor cortex excitability following short trains of repetitive magnetic stimuli. Exp Brain Res. 2001; 140(4):453–9. [PubMed: 11685398]
8. Fitzgerald PB, Brown TL, Daskalakis ZJ, et al. Intensity-dependent effects of 1 Hz rTMS on human corticospinal excitability. Clinical neurophysiology. 2002; 113(7):1136–1141. [PubMed: 12088710]
9. Peinemann A, Reimer B, Löer C, et al. Long-lasting increase in corticospinal excitability after 1800 pulses of subthreshold 5 Hz repetitive TMS to the primary motor cortex. Clinical neurophysiology. 2004; 115(7):1519–1526. [PubMed: 15203053]
10. Quartarone A, Rizzo V, Bagnato S, et al. Homeostatic-like plasticity of the primary motor hand area is impaired in focal hand dystonia. Brain. 2005; 128(Pt 8):1943–50. [PubMed: 15872016]
11. Fox P, Ingham R, George MS, et al. Imaging human intra-cerebral connectivity by PET during TMS. Neuroreport. 1997; 8(12):2787–91. [PubMed: 9295118]
12. Paus T, Jech R, Thompson CJ, et al. Transcranial magnetic stimulation during positron emission tomography: a new method for studying connectivity of the human cerebral cortex. The Journal of neuroscience. 1997; 17(9):3178–84. [PubMed: 9096152]
13. Siebner HR, Takano B, Peinemann A, et al. Continuous transcranial magnetic stimulation during positron emission tomography: a suitable tool for imaging regional excitability of the human cortex. NeuroImage. 2001; 14(4):883–90. [PubMed: 11554807]
14. Bestmann S, Baudewig J, Siebner HR, et al. Subthreshold high-frequency TMS of human primary motor cortex modulates interconnected frontal motor areas as detected by interleaved fMRI-TMS. NeuroImage. 2003; 20(3):1685–96. [PubMed: 14642478]

15. Speer AM, Willis MW, Herscovitch P, et al. Intensity-dependent regional cerebral blood flow during 1-Hz repetitive transcranial magnetic stimulation (rTMS) in healthy volunteers studied with H215O positron emission tomography: I. Effects of primary motor cortex rTMS. Biological psychiatry. 2003; 54(8):818–25. [PubMed: 14550681]
16. Rounis E, Lee L, Siebner HR, et al. Frequency specific changes in regional cerebral blood flow and motor system connectivity following rTMS to the primary motor cortex. NeuroImage. 2005; 26(1): 164–76. [PubMed: 15862216]
17. Allen EA, Pasley BN, Duong T, et al. Transcranial magnetic stimulation elicits coupled neural and hemodynamic consequences. Science (New York, NY). 2007; 317(5846):1918–21.
18. Sack AT, Kohler A, Bestmann S, et al. Imaging the Brain Activity Changes Underlying Impaired Visuospatial Judgments: Simultaneous fMRI, TMS, and Behavioral Studies. Cerebral cortex. 2007; 17(12):2841–2852. [PubMed: 17337745]
19. Bestmann S, Ruff CC, Blakemore C, et al. Spatial Attention Changes Excitability of Human Visual Cortex to Direct Stimulation. Current Biology. 2007; 17(2):134–139. [PubMed: 17240338]
20. George MS, Wassermann EM, Kimbrell TA, et al. Mood Improvement Following Daily Left Prefrontal Repetitive Transcranial Magnetic Stimulation in Patients With Depression: A Placebo-Controlled Crossover Trial. Am J Psychiatry. 1997; 154:1752–1756. [PubMed: 9396958]
21. O'Reardon JP, Solvason HB, Janicak PG, et al. Efficacy and Safety of Transcranial Magnetic Stimulation in the Acute Treatment of Major Depression: A Multisite Randomized Controlled Trial. Biological psychiatry. 2007; 62(11):1208–1216. [PubMed: 17573044]
22. Weiduschat N, Thiel A, Rubi-Fessen I, et al. Effects of repetitive transcranial magnetic stimulation in aphasic stroke: A randomized controlled pilot study. Stroke. 2011; 42(2):409–415. [PubMed: 21164121]
23. Naeser MA, Martin PI, Ho M, et al. Transcranial Magnetic Stimulation and Aphasia Rehabilitation. Archives of Physical Medicine and Rehabilitation. 2012; 93(1, Supplement):S26–S34. [PubMed: 22202188]
24. Mayberg HS, Liotti M, Brannan SK, et al. Reciprocal limbic-cortical function and negative mood: converging PET findings in depression and normal sadness. Am J Psychiatry. 1999; 156(5):675–82. [PubMed: 10327898]
25. Mayberg HS, Lozano AM, Voon V, et al. Deep Brain Stimulation for Treatment-Resistant Depression. Neuron. 2005; 45(5):651–660. [PubMed: 15748841]
26. Fox MD, Buckner RL, White MP, et al. Efficacy of Transcranial Magnetic Stimulation Targets for Depression Is Related to Intrinsic Functional Connectivity with the Subgenual Cingulate. Biological psychiatry. 2012 0):
27. Fox PT, Raichle ME. Stimulus rate dependence of regional cerebral blood flow in human striate cortex, demonstrated by positron emission tomography. Journal of neurophysiology. 1984; 51(5): 1109–20. [PubMed: 6610024]
28. Kwong KK, Belliveau JW, Chesler DA, et al. Dynamic Magnetic Resonance Imaging of Human Brain Activity During Primary Sensory Stimulation. Proceedings of the National Academy of Sciences of the United States of America. 1992; 89(12):5675–5679. [PubMed: 1608978]
29. Blood AJ, Narayan SM, Toga AW. Stimulus Parameters Influence Characteristics of Optical Intrinsic Signal Responses in Somatosensory Cortex. J Cereb Blood Flow Metab. 1995; 15(6): 1109–1121. [PubMed: 7593344]
30. Ibañez V, Deiber M-P, Sadato N, et al. Effects of stimulus rate on regional cerebral blood flow after median nerve stimulation. Brain. 1995; 118(5):1339–1351. [PubMed: 7496791]
31. Ngai AC, Jolley MA, D'Ambrosio R, et al. Frequency-dependent changes in cerebral blood flow and evoked potentials during somatosensory stimulation in the rat. Brain research. 1999; 837(1–2): 221–228. [PubMed: 10434006]
32. Matsuura T, Kanno I. Quantitative and temporal relationship between local cerebral blood flow and neuronal activation induced by somatosensory stimulation in rats. Neuroscience research. 2001; 40(3):281–290. [PubMed: 11448520]
33. Committee for the Update of the Guide for the Care, Use of Laboratory Animals, and National Research Council. Guide for the Care and Use of Laboratory Animals. The National Academies Press; Washington, D.C: 2011.

34. *Animal Welfare Act, 7 U.S.C. 54 § 2143*, 2009.
35. Szabó CA, Leland MM, Knape K, et al. Clinical and EEG phenotypes of epilepsy in the baboon (Papio hamadryas spp). Epilepsy research. 2005; 65(1–2):71–80. [PubMed: 15994062]
36. Wey H-Y, Li J, Szabó CÁ, et al. BOLD fMRI of visual and somatosensory-motor stimulations in baboons. NeuroImage. 2010; 52(4):1420–7. [PubMed: 20471483]
37. Woolrich MW, Jbabdi S, Patenaude B, et al. Bayesian analysis of neuroimaging data in FSL. NeuroImage. 2009; 45(1 Suppl):S173–86. [PubMed: 19059349]
38. Smith SM, Jenkinson M, Woolrich MW, et al. Advances in functional and structural MR image analysis and implementation as FSL. NeuroImage. 2004; 23(Suppl 1):S208–19. [PubMed: 15501092]
39. Penfield W, Boldrey E. Somatic motor and sensory representation in the cerebral cortex of man as studied by electrical stimulation. Brain. 1937; 60(4):389–443.
40. Salinas FS, Lancaster JL, Fox PT. Detailed 3D models of the induced electric field of transcranial magnetic stimulation coils. Phys Med Biol. 2007; 52(10):2879–92. [PubMed: 17473357]
41. Salinas FS, Lancaster JL, Fox PT. 3D modeling of the total electric field induced by transcranial magnetic stimulation using the boundary element method. Phys Med Biol. 2009; 54(12):3631–47. [PubMed: 19458407]
42. Chen R, Gerloff C, Classen J, et al. Safety of different inter-train intervals for repetitive transcranial magnetic stimulation and recommendations for safe ranges of stimulation parameters. Electroencephalography and clinical neurophysiology. 1997; 105(6):415–21. [PubMed: 9448642]
43. Wassermann EM. Risk and safety of repetitive transcranial magnetic stimulation: report and suggested guidelines from the International Workshop on the Safety of Repetitive Transcranial Magnetic Stimulation, June 5–7, 1996. Electroencephalography and clinical neurophysiology. 1998; 108(1):1–16. [PubMed: 9474057]
44. Rossi S, Hallett M, Rossini PM, et al. Safety, ethical considerations, and application guidelines for the use of transcranial magnetic stimulation in clinical practice and research. Clin Neurophysiol. 2009; 120(12):2008–39. [PubMed: 19833552]
45. Fox PT, Narayana S, Tandon N, et al. Intensity modulation of TMS-induced cortical excitation: primary motor cortex. Hum Brain Mapp. 2006; 27(6):478–87. [PubMed: 16161021]
46. Jenkinson M, Bannister P, Brady M, et al. Improved optimization for the robust and accurate linear registration and motion correction of brain images. NeuroImage. 2002; 17(2):825–41. [PubMed: 12377157]
47. Lancaster JL, Fox PT, Downs H, et al. Global spatial normalization of human brain using convex hulls. J Nucl Med. 1999; 40(6):942–55. [PubMed: 10452309]
48. Sack AT, Cohen Kadosh R, Schuhmann T, et al. Optimizing Functional Accuracy of TMS in Cognitive Studies: A Comparison of Methods. Journal of Cognitive Neuroscience. 2009; 21(2): 207–221. [PubMed: 18823235]
49. Guye M, Parker GJM, Symms M, et al. Combined functional MRI and tractography to demonstrate the connectivity of the human primary motor cortex in vivo. NeuroImage. 2003; 19(4):1349–60. [PubMed: 12948693]
50. Laird AR, Robbins JM, Li K, et al. Modeling motor connectivity using TMS/PET and structural equation modeling. NeuroImage. 2008; 41(2):424–36. [PubMed: 18387823]
51. Geyer S, Matelli M, Luppino G, et al. Functional neuroanatomy of the primate isocortical motor system. Anatomy and embryology. 2000; 202(6):443–74. [PubMed: 11131014]
52. Dum RP, Strick PL. Motor areas in the frontal lobe of the primate. Physiology & behavior. 2002; 77(4–5):677–82. [PubMed: 12527018]
53. Dum RP, Strick PL. Frontal lobe inputs to the digit representations of the motor areas on the lateral surface of the hemisphere. The Journal of neuroscience. 2005; 25(6):1375–86. [PubMed: 15703391]
54. Rizzolatti G, Luppino G. The cortical motor system. Neuron. 2001; 31(6):889–901. [PubMed: 11580891]
55. Matelli M, Carmada R, Glickstein M, et al. Interconnections within the postarcuate cortex (area 6) of the macaque monkey. Brain research. 1984; 310(2):388–92. [PubMed: 6488031]

56. Tanji J. The supplementary motor area in the cerebral cortex. Neuroscience research. 1994; 19(3): 251–68. [PubMed: 8058203]
57. Paus T. Primate anterior cingulate cortex: where motor control, drive and cognition interface. Nature reviews Neuroscience. 2001; 2(6):417–24.
58. Nachev P, Kennard C, Husain M. Functional role of the supplementary and pre-supplementary motor areas. Nature reviews Neuroscience. 2008; 9(11):856–69.
59. Saleem, KS.; Logothetis, NK. A combined MRI and histology atlas of the rhesus monkey brain in stereotaxic coordinates. Academic Press; London: 2007.
60. Pandya DN, Hoesen GWV, Mesulam MM. Efferent connections of the cingulate gyrus in the rhesus monkey. Experimental brain research. 1981; 42(3–4):319–30.
61. Fink GR. Multiple nonprimary motor areas in the human cortex. Journal of neurophysiology. 1997; 77(4):2164–74. [PubMed: 9114263]
62. Cavada C. The anatomical connections of the macaque monkey orbitofrontal cortex. A review. Cerebral cortex (New York, NY : 1991). 2000; 10(3):220–42.
63. Margulies DS, Vincent JL, Kelly C, et al. Precuneus shares intrinsic functional architecture in humans and monkeys. Proceedings of the National Academy of Sciences of the United States of America. 2009; 106(47):20069–74. [PubMed: 19903877]
64. Moisa M, Pohmann R, Uludaƒü K, et al. Interleaved TMS/CASL: Comparison of different rTMS protocols. NeuroImage. 2010; 49(1):612–620. [PubMed: 19615453]
65. Lee L, Siebner HR, Rowe JB, et al. Acute remapping within the motor system induced by low-frequency repetitive transcranial magnetic stimulation. J Neurosci. 2003; 23(12):5308–18. [PubMed: 12832556]
66. Di Lazzaro V, Oliviero A, Mazzone P, et al. Short-term reduction of intracortical inhibition in the human motor cortex induced by repetitive transcranial magnetic stimulation. Exp Brain Res. 2002; 147(1):108–13. [PubMed: 12373375]
67. Berardelli A, Inghilleri M, Rothwell JC, et al. Facilitation of muscle evoked responses after repetitive cortical stimulation in man. Experimental brain research. 1998; 122(1):79–84.
68. Buzsáki G, Draguhn A. Neuronal Oscillations in Cortical Networks. Science. 2004; 304(5679): 1926–1929. [PubMed: 15218136]
69. Thut G, Miniussi C. New insights into rhythmic brain activity from TMS-EEG studies. Trends in Neurosciences. 2009; 13(4):182.
70. Thut G, Veniero D, Romei V, et al. Rhythmic TMS Causes Local Entrainment of Natural Oscillatory Signatures. Current Biology. 2011; 21(14):1176–1185. [PubMed: 21723129]
71. Feurra M, Bianco G, Santarnecchi E, et al. Frequency-Dependent Tuning of the Human Motor System Induced by Transcranial Oscillatory Potentials. The Journal of neuroscience. 2011; 31(34): 12165–12170. [PubMed: 21865459]
72. Huang YZ, Edwards MJ, Rounis E, et al. Theta burst stimulation of the human motor cortex. Neuron. 2005; 45(2):201–6. [PubMed: 15664172]
73. Rothkegel H, Sommer M, Paulus W. Breaks during 5Hz rTMS are essential for facilitatory after effects. Clinical neurophysiology. 2010; 121(3):426–430. [PubMed: 20006546]
74. Långsjö JK, Kaisti KK, Aalto S, et al. Effects of subanesthetic doses of ketamine on regional cerebral blood flow, oxygen consumption, and blood volume in humans. Anesthesiology. 2003; 99(3):614–23. [PubMed: 12960545]
75. Wey H-Y, Wang DJ, Duong TQ. Baseline CBF, and BOLD, CBF, and CMRO(2) fMRI of visual and vibrotactile stimulations in baboons. Journal of cerebral blood flow and metabolism. 2011; 31(2):715–24. [PubMed: 20827260]
76. Salinas, FS.; Narayana, S.; Zhang, W., et al. Baboon Validations of the cortical column cosine aiming model of TMS induced brain activations. 17th Annual Meeting of the Organization for Human Brain Mapping; Quebec City, Canada. 2011; June 26–30;
77. Salinas, FS.; Narayana, S.; Zhang, W., et al. Investigating the mechanisms of transcranial magnetic stimulation in a baboon model. 41st Annual Meeting of the Society for Neuroscience; Washington DC. 2011; November 12–16;

78. Salinas, FS.; Narayana, S.; Zhang, W., et al. Baboon Validations of the Cortical Column TMS Aiming Strategy: CBF dependence on Coil Orientation. 18th Annual Meeting of the Organization for Human Brain Mapping; Beijing, China. 2012; June 10–14;

79. Salinas, FS.; Narayana, S.; Jimenez-Castro, L., et al. Resting-state fMRI determination of optimal target locations for non-invasive brain stimulation. 42nd Annual Meeting of the Society for Neuroscience; New Orleans. 2012; October 13–17;

80. Vincent JL, Patel GH, Fox MD, et al. Intrinsic functional architecture in the anaesthetized monkey brain. Nature. 2007; 447(7140):83–6. [PubMed: 17476267]

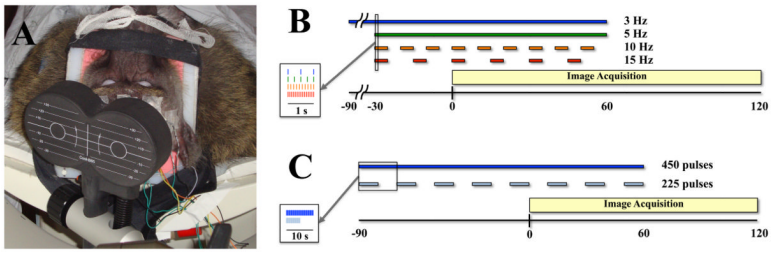

Figure 1.

rTMS/PET stimulation. **A.** Baboon positioned in a custom head/shoulder restraint during rTMS/PET. rTMS was performed at frequencies of 3 Hz, 5 Hz, 10 Hz and 15 Hz with a limited scalp EEG montage. Image reprinted with permission from Salinas *et al.*, 2011.[5] **B.** Stimulation protocol for delivering rTMS frequencies at 3 Hz, 5 Hz, 10 Hz and 15 Hz. The number of stimuli were limited to 450 total TMS pulses, with 5 Hz, 10 Hz, and 15 Hz rTMS applied for a total of 90 seconds (3 Hz rTMS was delivered for 150 seconds). The 3 Hz and 5 Hz rTMS frequencies were delivered continuously, whereas the train durations of the 10 Hz and 15 Hz stimulations were adjusted so that all of the pulses at that frequency were given over the 90 second rTMS period. Limiting the number of pulses (especially at higher rTMS frequencies) has the added benefit of reducing coil heating effects due to our long train durations at suprathreshold rTMS intensities. **B.** Stimulation protocol for testing the effect of the number of stimuli delivered. rTMS was delivered at 3 Hz using both continuous (450 pulses) and intermittent (225 pulses) pulse trains for a total period of 150 seconds. Radioisotope injection occurred at the “0” second timepoint in each scan.

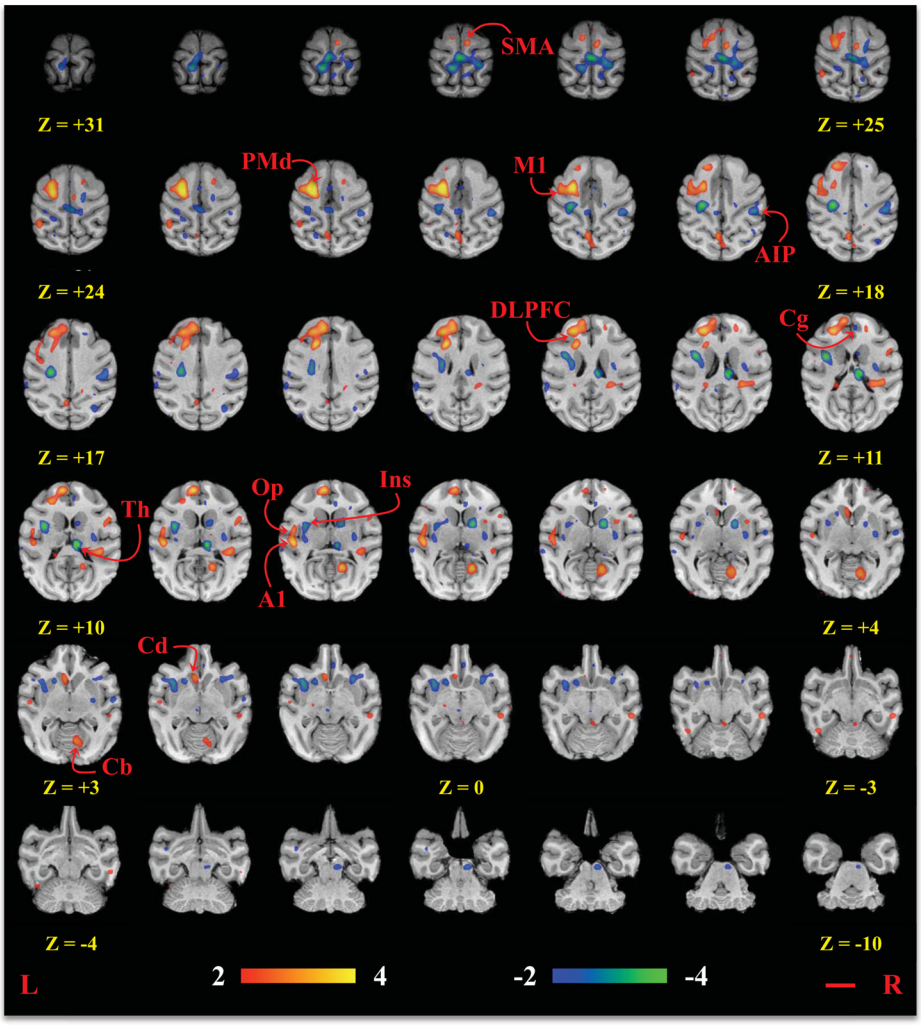

Figure 2.

Statistical parametric images of all rTMS frequencies (compared to rest). All coordinates are relative to the anterior commissure, which is located at (0 mm, 0 mm, 0 mm). The red line represents a 1 cm distance. M1 = primary motor cortex; PMd = dorsal premotor cortex; SMA = supplementary motor area; Cg = cingulate motor area; Cd = caudate; Th = thalamus; Cb = cerebellum; DLPFC = dorsolateral prefrontal cortex; Ins = insular cortex; Op = parietal operculum; AIP = anterior intraparietal sulcus; A1 = primary auditory cortex.

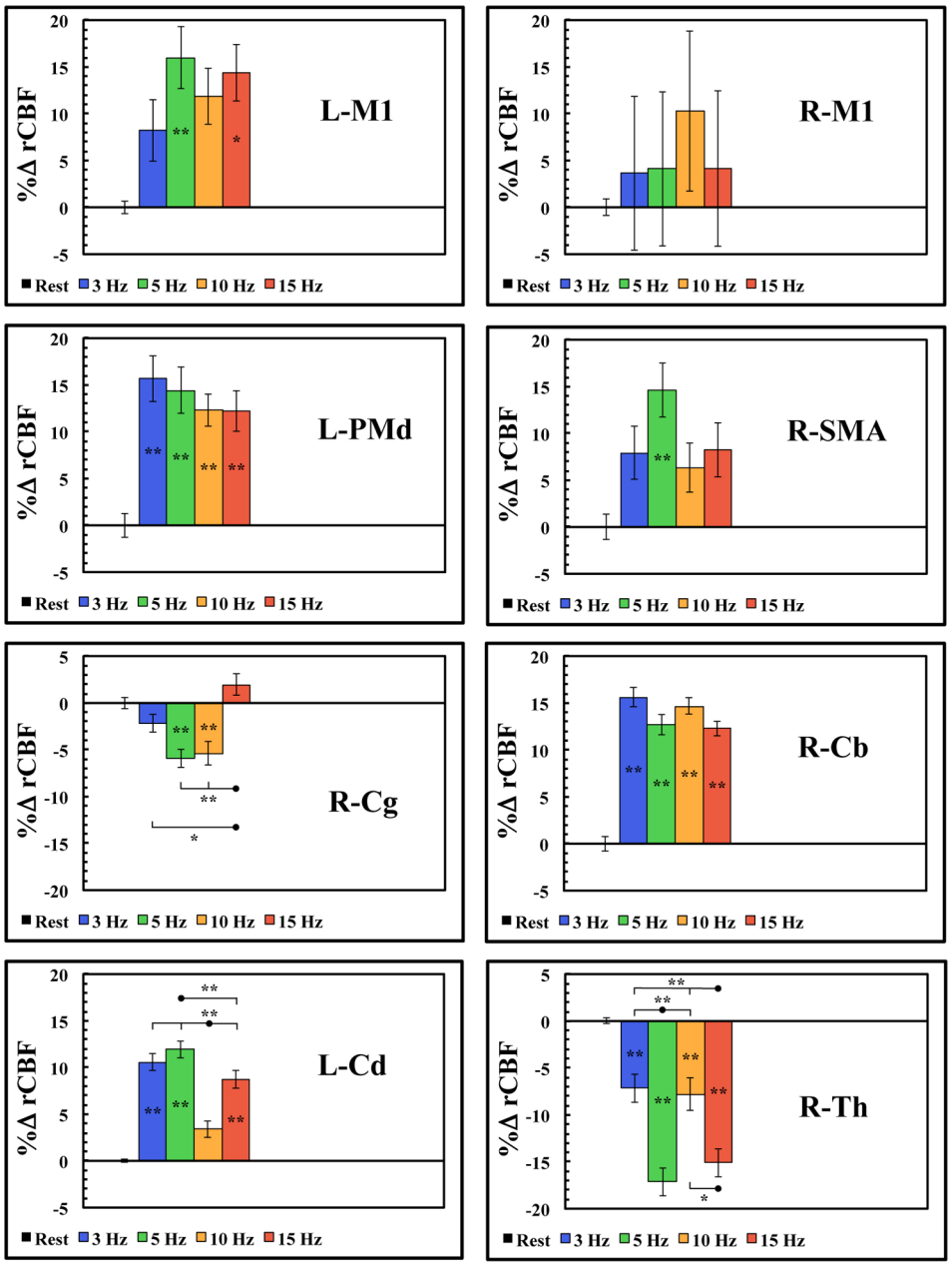

Figure 3.

ROI analysis (mean ± SEM) of the motor areas activated during rTMS of the L-M1. L= left; R = right; M1 = primary motor cortex; PMd = dorsal premotor cortex; SMA = supplementary motor area; Cg = cingulate motor area; Cd = caudate; Th = thalamus; Cb = cerebellum; (*$p < 0.05$; **$p < 0.01$).

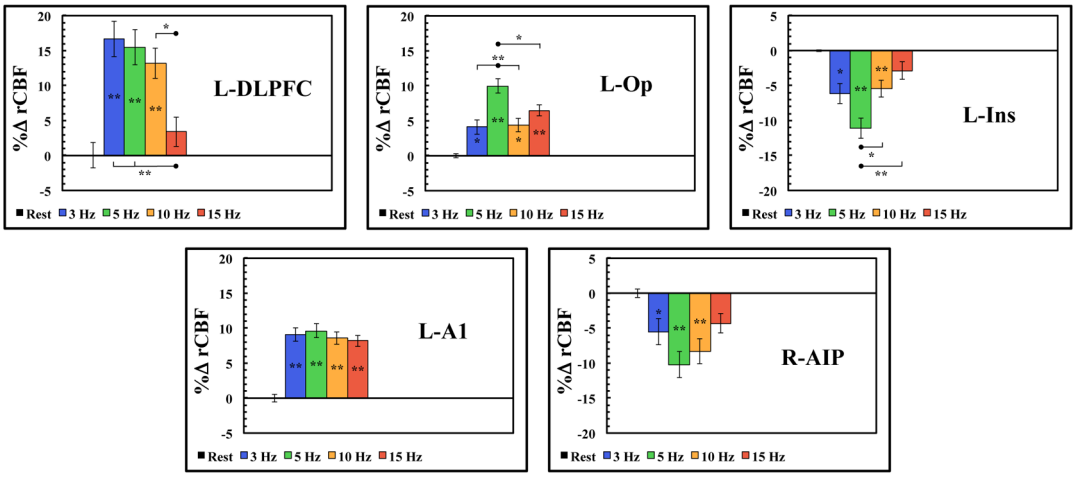

Figure 4.

ROI analysis (mean ± SEM) of non-motor areas activated during rTMS of the L-M1. L= left; R = right; DLPFC = dorsolateral prefrontal cortex; Ins = insular cortex; Op = parietal operculum; AIP = anterior intraparietal sulcus; A1 = primary auditory cortex; (*$p < 0.05$; **$p < 0.01$).

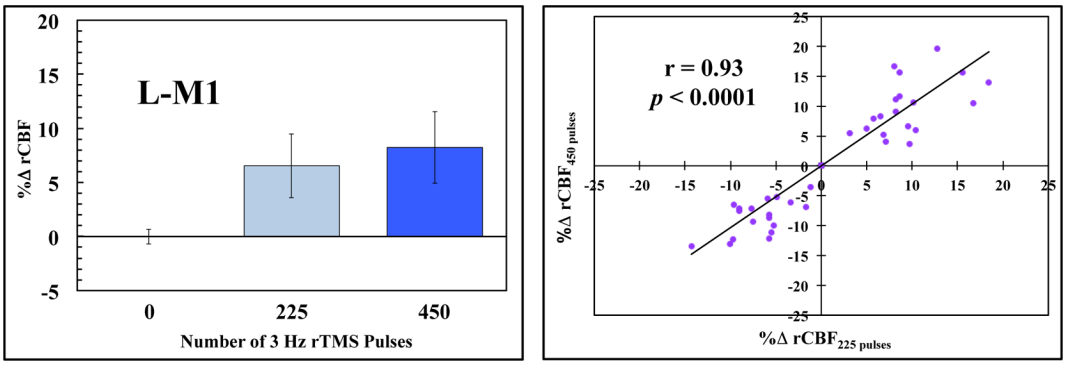

Figure 5.

Comparison of continuous and intermittent rTMS pulses on regional CBF. **A.** ROI analysis (mean ± SEM) of L-M1 for continuous (450 pulses) and intermittent (225 pulses) delivery of 3 Hz rTMS pulses. **B.** Linear regression of all the sites listed in Table 1 at 3 Hz rTMS. This supports the notion that we are examining an intrinsic frequency response of the motor system, rather than the cumulative effect of stimuli bombarding the system.

Table 1

Regions of brain activity during rTMS compared to the baseline condition (N = 5).

	Region of Interest	Area*	Coordinates** (mm)			Volume (mm^3)	Z-score	p-value
			x	y	z			
Ipsilateral	§ Dorsal precentral	F1	−19	−1	20	680	3.13	0.0007
	Dorsal premotor	F2	−13	0	22	1000	5.04	p<0.00003
	Prearcuate gyrus	DLPFC	−13	17	13	992	3.82	0.0001
	Superior frontal gyrus	Area 9m	−5	25	9	968	3.76	0.0001
	Parietal operculum	SII	−26	−4	8	664	2.79	0.0027
	Insular cortex	Ial	−19	7	1	880	−3.18	0.0007
	Insular cortex	Ig	−18	−10	8	384	−2.40	0.0082
	Temporal pole	TGvd	−16	5	−16	536	−2.53	0.0058
	Auditory Cortex	A1	−26	−12	8	864	3.756	0.00009
	Ventral intraparietal area	VIP	−14	−12	18	992	−4.09	p<0.00003
	Superior temporal sulcus	Area TAa	−31	−22	14	536	−2.53	0.0058
	Postcentral gyrus	Areas 1–2	−6	−21	29	952	−3.43	0.0003
	Inferior parietal lobule	Area 7a	−21	−25	24	688	3.04	0.0012
	Superior temporal sulcus	Area TAa	−31	−22	14	536	−2.53	0.0058
	Medial preoccipital gyrus	Area PO	−3	−33	19	736	3.04	0.0012
	Caudate nucleus	-	−4	11	2	712	2.97	0.0015
	Putamen	-	−11	8	1	664	−2.90	0.0019
Contralateral	Dorsal premotor	F2	9	5	23	272	2.51	0.0061
	Superior frontal gyrus	SMA	3	5	28	560	2.97	0.0015
	Anterior cingulate cortex	Area 24b	3	15	11	328	−2.46	0.0069
	Dorsal precentral gyrus	F1	9	−7	25	568	−2.84	0.0023
	Postcentral gyrus	Areas 3a/b	26	3	10	504	2.66	0.0039
	Postcentral gyrus	Areas 1–2	31	−5	4	496	−2.74	0.0031
	Superior frontal gyrus	Area 9d	10	19	12	280	2.63	0.0043
	Insular cortex	Iapl	16	9	1	704	−2.78	0.0028
	Insular cortex	Ig	17	−8	9	752	−2.59	0.0049
	Postcentral gyrus	Areas 1–2	0	−14	27	984	−3.81	0.0001

Region of Interest	Area*	Coordinates** (mm)			Volume (mm^3)	Z-score	p-value
		x	y	z			
Anterior intraparietal sulcus	AIP	23	−16	19	864	−2.96	0.0015
Middle temporal gyrus	Areas TEm	28	−16	−2	648	2.57	0.0051
Postcentral gyrus	Areas 1–2	9	−17	26	800	−2.93	0.0017
Superior parietal lobule	Area 5	13	−19	28	784	−3.18	0.0007
Occipital gyrus	V2	8	−30	7	904	3.47	0.0003
Cerebellum	Cblm	21	−18	3	872	3.01	0.0013
Internal capsule	IC	9	1	6	872	−3.68	0.0001
Putamen	-	16	−6	5	576	−2.56	0.0053
Thalamus	-	5	−13	10	992	−4.56	p<0.00003
Pons	-	4	−13	−7	584	−2.78	0.0028

*Labels correspond to the homologous areas listed in the rhesus[59]

**Coordinates are relative to the anterior commissure (0 mm, 0 mm, 0 mm)

§Targeted primary motor cortex

Brain Stimul. Author manuscript; available in PMC 2014 September 01.

Table 2

Repeated-measures one-way ANOVA values for each frequency experiment.

Region of Interest	$F_{4,20}$	*p*-value
L-M1	15.54	6.25×10^{-6}
R-M1	0.64	6.42×10^{-1}
Premotor	12.10	3.68×10^{-5}
SMA	5.65	3.29×10^{-3}
Anterior Cingulate	11.87	4.20×10^{-5}
Cerebellum	48.62	5.00×10^{-10}
Caudate	116.28	1.50×10^{-13}
Thalamus	63.68	4.30×10^{-11}
DLPFC	12.16	3.58×10^{-5}
Parietal Operculum	34.15	1.12×10^{-8}
Insula	32.27	1.83×10^{-8}
A1	26.62	9.21×10^{-8}
Anterior Intraparietal Area	11.56	5.03×10^{-5}